

Parallel Implementation of Spatial Pooler in Hierarchical Temporal Memory

Marcin Pietron^{1,2}, Maciej Wielgosz^{1,2} and Kazimierz Wiatr^{1,2}

¹AGH University of Science and Technology, Mickiewicza 30, 30-059, Cracow, Poland

²ACK Cyfronet AGH, Nawojki 11, 30-950, Cracow, Poland

Keywords: Artificial Intelligence, GPGPU Computing, Hierarchical Temporal Memory, Machine Learning, Neocortex.

Abstract: Hierarchical Temporal Memory is a structure that models some of the structural and algorithmic properties of the neocortex. HTM is a biological model based on the memory-prediction theory of brain. HTM is a method for discovering and learning of observed input patterns and sequences, building an increasingly complex models. HTM combines and extends approaches used in sparse distributed memory, bayesian networks, spatial and temporal clustering algorithms, using a tree-shaped hierarchy neural networks. It is quite a new model of deep learning process, which is very efficient technique in artificial intelligence algorithms. HTM like other deep learning models (Boltzmann machine, deep belief networks etc.) has structure which can be efficiently processed by parallel machines. Modern multi-core processors with wide vector processing units (SSE, AVX), GPGPU are platforms that can tremendously speed up learning, classifying or clustering algorithms based on deep learning models (e.g. Cuda Toolkit 7.0). The current bottleneck of this new flexible artificial intelligence model is efficiency. This article focuses on parallel processing of HTM learning algorithms in parallel hardware platforms. This work is the first one about implementation of HTM architecture and its algorithms in hardware accelerators. The article doesn't study quality of the algorithm.

1 INTRODUCTION

Nowadays, a huge amount of data is generated by millions of sources in the Internet domain at any given time. It is estimated that all the data collected in 2012 from the Internet amounted to 2.7 ZB, which is a 48% increase compared to 2011; at the end of 2013, this number reached 4 ZB (Idc, 2011) (Hilbert and Lopez, 2011). Furthermore, the amount of data transferred within the areas of telecommunication networks grows with an increase in the number of data sources. In 2010 it was 14 EB, in 2011 - 20 EB, in 2012 - 31 EB per month in non-mobile networks (Cisco, 2012). There is a similar rate of growth in the mobile infrastructure in the year 2010 - 256 PB, 2011 - 597 PB and 2012 - 885 PB per month (Cisco, 2012). It is expected that the coming years will witness a further increase in the number of mobile devices and other data sources, which will result in continued exponential growth of data generation.

Storing all the data (raw data) requires a huge amount of disk space. In addition, with the development of network infrastructure and increase in the amount of available data, the demand for precise in-

formation and fast data analysis is rising. Therefore, it can be expected that in the future, carefully extracted information will be stored in a well-defined model of self-adaptive architecture (Hawkins and Ahmad, 2011)(Wu et al., 2014), which will also be used for advanced context-sensitive filtering of incoming data.

Nowadays, virtually all the companies and institutions need reliable information which should be rapidly accessible. This is very often a decisive factor when it comes to a company's evolution and its survival on the market. For example, companies in the banking sector are especially concerned about an access to up-to-date, reliable information. Sometimes a couple of seconds makes a huge difference and decides about profit or loss which, in the long run, affects the whole performance of the institution. Consequently, there is a need to develop systems capable of extracting knowledge from many incoming data streams quickly and accurately. To operate effectively, such systems should be equipped with well-designed algorithms that enable modeling of a selected area of knowledge in real time (adding new and removing old outdated structures) and the appropriate hardware infrastructure allowing for fast data processing (Cai

et al., 2012) (Lopes et al., 2012).

In many state-of-the-art content extraction systems, a classifier is trained, and the process demands a large set of training vectors. The vectors are extracted from the database and the training is performed. This operation may be regarded as the creation of an initial model of the extracted knowledge. In order to change the model, that process must be performed again, which is time consuming and can not always be performed in real time. There are different kinds of classifiers used in the information extraction systems such as SVM, K-means, Bayesian nets, Boltzmann Machine etc. There are also various methods of matrix reduction employed in order to reduce the computational complexity and keep the quality of the comparison results at the same high level. The most popular and frequently used algorithms for matrix dimensionality reduction are PCA and SVD. Standard implementations of those algorithms are highly iterative and sequential by their nature, which means that they require a substantial number of sequential steps to reduce a matrix.

An alternative to the conventional methods are algorithms based on sparse distributed representation and Hierarchical Temporal Memory, which store the contextual relationships between data rather than bare data value, as the dense representation (Hawkins and Ahmad, 2011). It can be thought of as a semantic map of the data, so the conversion from dense to sparse representation is a transition from a description in words and sentences into description in semantic maps which can be processed at the pixel level. In the case of sparse distributed representation, every bit has a semantic meaning. Therefore, mapping to the sparse distributed representation is a very important stage (Fig. 1).

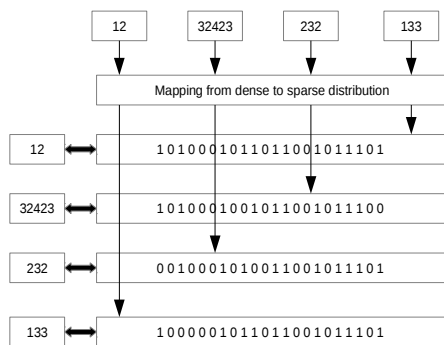


Figure 1: Dense to sparse data representation mapping.

2 GPGPU AND MULTIPROCESSOR COMPUTING

The architecture of a GPGPU card is described in Fig. 2. GPGPU is constructed as N multiprocessor structure with M cores each. The cores share an Instruction Unit with other cores in a multiprocessor. Multiprocessors have dedicated memory chips which are much faster than global memory, shared for all multiprocessors. These memories are: read-only constant/texture memory and shared memory. The GPGPU cards are constructed as massive parallel devices, enabling thousands of parallel threads to run which are grouped in blocks with shared memory. A dedicated software architecture CUDA makes possible programming GPGPU using high-level languages such as C and C++ (NVIDIA, 2014). CUDA requires an NVIDIA GPGPU like Fermi, GeForce 8XXX/Tesla/Quadro etc. This technology provides three key mechanisms to parallelize programs: thread group hierarchy, shared memories, and barrier synchronization. These mechanisms provide fine-grained parallelism nested within coarse-grained task parallelism.

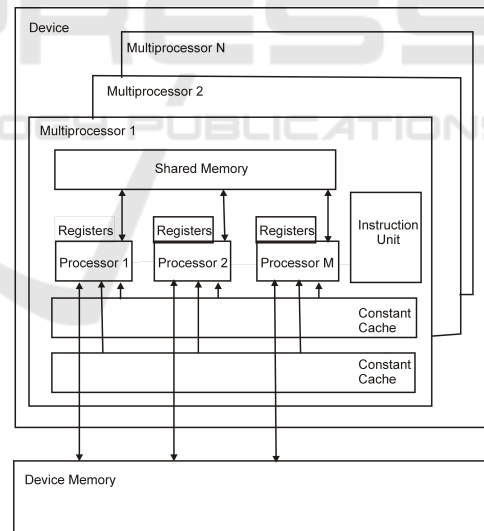


Figure 2: GPGPU architecture.

Creating the optimized code is not trivial and thorough knowledge of GPGPU's architecture is necessary to do it effectively. The main aspects to consider are the usage of the memories, efficient division of code into parallel threads and thread communications. As it was mentioned earlier, constant/texture, shared memories and local memories are specially optimized regarding the access time, therefore programmers should optimally use them to speedup access to

data on which an algorithm operates. Another important thing is to optimize synchronization and the communication of the threads. The synchronization of the threads between blocks is much slower than in a block. If it is not necessary it should be avoided, if necessary, it should be solved by the sequential running of multiple kernels. Another important aspect is the fact that recursive function calls are not allowed in CUDA kernels. Providing stack space for all the active threads requires substantial amounts of memory.

Modern processors consist of two or more independent central processing units. This architecture enables multiple CPU instructions (add, move data, branch etc.) to run at the same time. The cores are integrated into a single integrated circuit. The manufacturers AMD and Intel have developed several multi-core processors (dual-core, quad-core, hexa-core, octa-core etc.). The cores may or may not share caches, and they may implement message passing or shared memory inter-core communication. The single cores in multi-core systems may implement architectures such as vector processing, SIMD, or multi-threading. These techniques offer another aspect of parallelization (implicit to high level languages, used by compilers). The performance gained by the use of a multi-core processor depends on the algorithms used and their implementation.

There are lot of programming models and libraries of multi-core programming. The most popular are pthreads, OpenMP, Cilk++, TDD etc. In our work OpenMP was used (OpenMP, 2010), being a software platform supporting multi-threaded, shared-memory parallel processing multi-core architectures for C, C++ and Fortran languages. By using OpenMP, the programmer does not need to create the threads nor assign tasks to each thread. The programmer inserts directives to assist the compiler into generating threads for the parallel processor platform.

3 HIERARCHICAL TEMPORAL MEMORY

Hierarchical Temporal Memory (HTM) replicates the structural and algorithmic properties of the neocortex. It can be regarded as a memory system which is not programmed and it is trained through exposing them to data i.e. text. HTM is organized in the hierarchy which reflects the nature of the world and performs modeling by updating the hierarchy. The structure is hierarchical in both space and time, which is the key in natural language modeling since words and sentences come in sequences which describe cause and effect relationships between the latent objects. HTMs

may be considered similar to Bayesian Networks, HMM and Recurrent Neural Networks, but they are different in the way hierarchy, model of neuron and time is organized (Hawkins and Ahmad, 2011).

At any moment in time, based on current and past input, an HTM will assign a likelihood that given concepts are present in the examined stream. The HTM's output constitutes a set of probabilities for each of the learned causes. This moment-to-moment distribution of possible concepts (causes) is denoted as a belief. If the HTM covers a certain number of concepts it will have the same number of variables representing those concepts. Typically HTMs learn about many causes and create a structure of them which reflects their relationships.

Even for human beings, discovering causes is considered to be a core of perception and creativity, and people through course of their life learn how to find causes underlying objects in the world. In this sense HTMs mimic human cognitive abilities and with a long enough training, proper design and implementation, they should be able to discover causes humans can find difficult or are unable to detect (Kapuscinski, 2010)(Sherwin and Mavris, 2009).

HTM infers concepts of new stream elements and the result is a distribution of beliefs across all the learned causes. If the concept (e.g. one of the categories occurring in the examined stream) is unambiguous, the belief distribution will be peaked otherwise it will be flat. In HTMs it is possible to disable learning after training and still do inference.

4 SPATIAL POOLER IN HIERARCHICAL TEMPORAL MEMORIES

This paper focuses on spatial pooler parallelization. It may be summarized in the following steps:

- Starts with an input consisting of a fixed number of bits which could be sensory data or they could come from another region lower in the hierarchy,
- assigns a fixed number of columns in the region this entry. Each column has an associated segment of dendrites (Hawkins and Ahmad, 2011). Dendrite segments have potential synapses. Each synapse has a permanence value,
- determines number of valid synapses connected to every column,
- boosting factor is used to amplify value of columns. It is evaluated on the base of a given column neighbours,

- the columns which are selected by the boosting procedure inhibit all the neighbours within the inhibition radius,
- all the active columns have their synapses' permanence values adjusted. The ones aligned with active inputs are increased.

The detailed implementation of the algorithm is as follows:

- Each column is connected by a fixed number of inputs to randomly selected node inputs. Based on the input pattern, some columns will receive more active input values,
- Inputs of columns (synapses) have values (floating point between 0 and 1 called permanence value) which represents possibility of activating the synapse (if the value is greater than 0.5 and corresponding input is 1 the synapse is active),
- Columns which have more active connected synapses than given threshold (`minOverlap`) and its overlap parameter (number of active synapses) is better than k-th overlap of set of columns in spectrum of inhibition radius,
- During learning process columns gather information about their history of activity, overlap values (if overlap was greater than `minOverlap` or not), compute minimum and maximum overlap duty cycle and then decides according to the combinations of these parameters if their permanence values or inhibition radius should be changed.

Generally, spatial pooling selects a relatively constant number of the most active columns and inactivates (inhibits) other columns in the vicinity of the active ones. Similar input patterns tend to activate a stable set of columns. The classifier module based on Spatial Pooler is realized by overlap and activation computing on incoming input values. The rest of the parameters are set during learning process. The functionality of Spatial Pooler is similar to LVQ or Self Organizing Maps neural models.

5 IMPLEMENTATION OF SPATIAL POOLER IN GPGPU

This section describes GPU implementation of spatial pooler. As mentioned in previous section special data structures are needed for spatial algorithm. Mapping these data structures to GPU memory hierarchy is crucial for effective implementation. The permanence values, column inputs connections, column activation, `overlapDutyCycle`, `activeDutyCycle`,

minimum and maximum `overlapDutyCycle` are column local data structures (see algorithm in section 4). The overlap, `overlapDutyCycle`, `activeDutyCycle`, input data are shared between columns. The representation of data structures is crucial in efficient algorithm implementation. Some of the data like activation, values in `overlapDutyCycle` and `activeDutyCycle` arrays can be represented as a single bit. The representation width of the rest of the data depends on architecture of spatial pooler e.g. number of inputs of each column, ratio between number of columns and input size etc. The size of representation of data mentioned above were computed for our simulations as follows:

- `overlap`, `overlap DutyCycle`, `active DutyCycle` values are stored as array of integers, array size is equal to $blockDim.x \cdot nrOfColumnsPerThread$,
- input values for block columns in array of size $sizeOfInputPerBlock$, which is equal to $(2 \cdot radiusOfColumnInputs \cdot blockDim.x \cdot noOfColumnsPerThread + 2 \cdot radiusOfColumnInputs) \div 32$ (where $radiusOfColumnInputs$ is width of input where single column can be connected). Dividing by 32 due to fact that each single input signal is represented by single bit,
- activation as single bit or byte (depends on configuration),
- `overlap window`, `activation window` arrays as integer values with single bits inside representing if column was overlapped or activated in last 32 previous cycles,
- `minimum DutyCycle`, `maximum DutyCycle` as arrays of float values, array size is equal to $nrOfColumnsPerThread$,
- column connections inputs indexes as byte arrays (size equal to $nrOfColumnsPerThread \cdot noCollInputs$), permanence values as float arrays ($nrOfColumnsPerThread \cdot noCollInputs$)
- positions of central indexes column inputs store in integer arrays of size $nrOfColumnsPerThread$.

The Tesla M2090 has 48kB of shared memory per each block and 32kB register memory which can be divided between block threads. In our work three different configurations were implemented (each configuration run with 64 threads per block):

- thread processing one column with majority of local column data (column data not shared between other columns) stored in registers (minority in local thread memory), $radiusOfColumnInputs$ is 128, each column has 32 input connections, where all local column data stored in registers, shared data in block shared memory, the size

of data in local thread memory is: $(32 + 32 \cdot 4)$, the data in registers: $6 \cdot 4 + 1$ as six four bytes values are stored and one byte for activation, the size of data in shared memory is $(3 \cdot 4 \cdot \text{blockDim.x} + \text{sizeOfInputPerBlock})$, which is equal in our case $(12 \cdot 64 + (2 \cdot 32 \cdot 64 + 2 \cdot 32) \div 32)$ (figure 3),

- thread processing eight columns with local column data stored in local memory and registers, $\text{radiusOfColumnInputs}$ is 128, each column has 32 input connections, shared data of size $(3 \cdot 4 \cdot \text{blockDim} + \text{sizeOfInputPerBlock})$ in shared memory, the size of data in thread local memory is: $5 \cdot 4 \cdot 8 + 8 \cdot 32 \cdot (1 + 4)$, the data in registers: $1 + 4$, the size of data in shared memory is the same as in previous configuration (figure 4),
- thread processing eight columns with shared data filled as much as possible, only column inputs indexes, their permanence values are stored in local memory, the size of data in local memory is: $8 \cdot 32 \cdot (1 + 4)$, the data in registers: $1 + 4$, the size of data in shared memory is sum of $(3 \cdot 4 \cdot \text{blockDim} + \text{sizeOfInputPerBlock})$ and $5 \cdot 4 \cdot 8$.

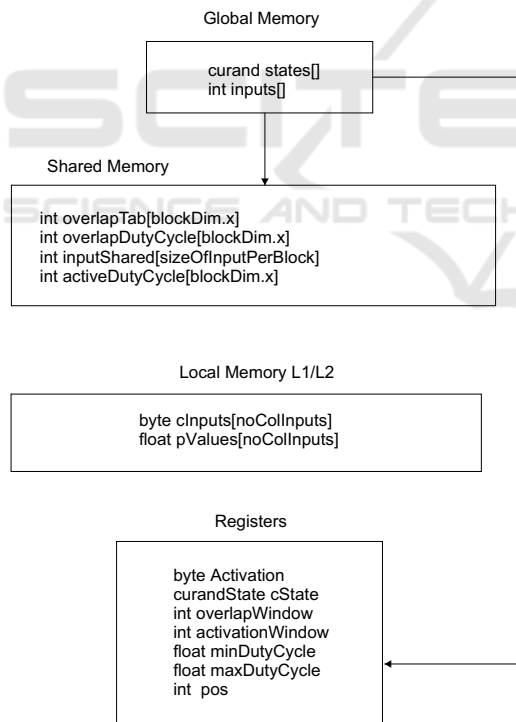


Figure 3: HTM architecture in GPU for 1 column processed by thread.

Random seed generator is stored always in registers. The main goal is to parameterized spatial pooler that as much as possible local column data fit available registers and local memory for single

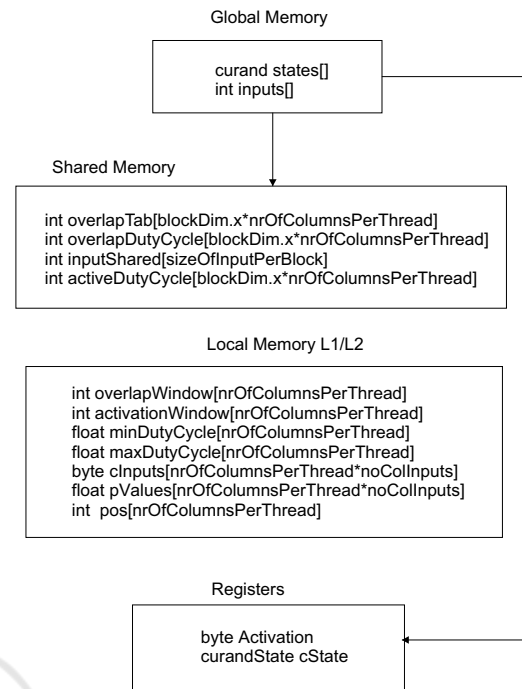


Figure 4: HTM architecture in GPU for 8 columns processed by thread.

block thread. The shared data should fit shared block memory. The shared data should be allocated in such manner that avoids bank conflicts (threads single instruction should read or write data from different banks). The input data stored in shared memory is the only one array with random access patterns and there is no way to avoid bank conflicts while its reading. The input signals represented by bits significantly decrease memory requirements. The algorithm in GPGPU firstly initializes by separate kernel initialize *curand* random generator and stores the seeds in global memory. Then HTM kernel reads in coalesced manner input values and seed from global memory and stores them in shared memory and registers, respectively. After that initializing column process is executed (random starting permanence values and connection indexes are generated and stored in local memory, figure 4 and figure 3). Then whole learning algorithm is executed (cycles of computing overlap, activation, permanence values updated, dutyCycle functions) on data stored in GPU memories. The columns processed by boundary threads (first thread and thread with $\text{blockDim.x}-1$ indexes) are processed with limited data because of the lack of values of all columns parameters in spectrum of inhibition radius (boundary effects due to shared and local memory parameters storing). In case of statistical algorithm like HTM spatial pooler this effect does not have negative influence on algorithm quality. Advantage

of storing data in shared memory during execution of whole algorithm is lack of global synchronization between blocks which in case of GPU is time consuming. The global synchronization can be solved by multi kernel invocation but it needs additional global store and write operations which significantly drops the efficiency. As was mentioned in previous section the classifier module is realized by just implemented overlap and activation functions. The input data is transferred from global memory (*sizeOfInputShared* for each block) in each cycle of classifying process.

6 IMPLEMENTATION OF SPATIAL POOLER IN OPENMP

As was mentioned in section 3, programmer by inserting openmp directives in appropriate places let compiler to parallelize the code. The spatial pooler algorithm can be divided to four main sections: column overlap computing, column activity checking, permanence values updates and DutyCycles parameter computation (Hawkins and Ahmad, 2011). All these sections are inside while loop are responsible for learning cycles processing. The iterations of while loop are dependent. All sections mentioned above apart from while loop can be fully parallelized. Therefore omp parallel for directive was used. After each section a thread barrier is automatically inserted. The pseudocode of openmp implementation is as follows:

```
while (cycle < nr_cycle) {
    #pragma omp parallel for
    for (nr = 0; nr < nrOfColumns; nr++) {
        overlapTab[nr]=overlap(nr)
    }
    #pragma omp parallel for
    for (nr = 0; nr < nrOfColumns; nr++) {
        activation[nr]=checkActivation(nr)
    }
    #pragma omp parallel for
    for (nr = 0; nr < nrOfColumns; nr++) {
        if (activation[nr] == 1)
            permValueUpdate(nr)
    }
    #pragma omp parallel for
    for (nr=0; nr < nrOfColumns; nr++) {
        activeDutyCycle[nr] = \
        computeActiveDutyCycle(nr)
        maxDutyCycle = computeMaxDutyCycle()
        minDutyCycle = computeMinDutyCycle()
        overlapDutyCycle[nr] = \
        overlapDutyCycle(nr)
    }
    cycle++
}
```

Table 1: Profiling of spatial pooler learning algorithm in CPU.

Method	percentage of whole algorithm execution
column initialization	2.5
overlap	28.4
activation	38.7
permanence values update	5
activeDutyCycle	8.5
overlapDutyCycle	9

Table 2: Profiling of spatial pooler learning algorithm in CPU for overlap and activation (*noOfColumns* \times *noOfColInputs* \times *inhibitionRadius*).

Configuration	overlap	activation
8192 \times 32 \times 32	28.4	38.7
8192 \times 32 \times 64	20.5	52.4
4096 \times 64 \times 32	37	29.6
16384 \times 16 \times 32	25.9	34.4

Table 3: Profiling of spatial pooler learning algorithm in CPU for permanence update and total time (*noOfColumns* \times *noOfColInputs* \times *inhibitionRadius*).

Configuration	permanence update	total time (ms)
8192 \times 32 \times 32	5	397
8192 \times 32 \times 64	2	570
4096 \times 64 \times 32	5.5	270
16384 \times 16 \times 32	4.2	593

7 EXPERIMENTAL RESULTS

Tables 1, 2 and 3 present results of profiling learning algorithm of spatial pooler. It is worth noting that execution time varies significantly across code sections. Activation computing is almost the most computationally exhaustive. However, the proportions may change for different set-up parameters. This applies in particular to the overlap computation since it is the second most computationally demanding section. The rest of the functions like *minOverlapDutyCycle*, *maxDutyCycle*, *boost* and *inhibitionRadius* update are omitted in tables because their contribution in whole time is negligible. As profiled data and time of execution of learning algorithm is known it is possible to estimate efficiency of pattern classifier based on Spatial Pooler (see section 4).

Then experimental tests of learning spatial pooler algorithm were run. Results were measured with different parameters. Tables 4 and 5 describe results gained in Python (1 core CPU, like in NuPic (Numenta, 2011)), GPU, single and multicore CPU

Table 4: Execution times of 100 cycles learning algorithm in SP on CPU (1 core) and GPU (miliseconds).

Input size (no.columns)	Python 1 core	GPGPU	C/C++ 1 core
2^{23} (2^{17})	855190	31.4	21019
2^{22} (2^{16})	413310	15.0	10250
2^{21} (2^{15})	205400	8.4	4100
2^{20} (2^{14})	103270	5.5	2590

Table 5: Execution times of 100 cycles learning algorithm in SP on CPU with vectorized version (miliseconds).

Input size (no.columns)	CPU (1 core) (vectorized)	CPU (6 cores) (vectorized)
2^{23} (2^{17})	5160	1419
2^{22} (2^{16})	2555	692
2^{21} (2^{15})	1255	361
2^{20} (2^{14})	613	178

Table 6: Execution times of 100 cycles learning algorithm in SP in two different GPU configurations (miliseconds).

Input size (no.columns)	1 column per thread	8 columns per thread
2^{23} (2^{17})	154.2	31.4
2^{22} (2^{16})	69.9	15.0
2^{21} (2^{15})	33	8.4
2^{20} (2^{14})	16.32	5.5

Table 7: Execution times of 100 cycles learning algorithm in SP in full shared memory GPU configuration (miliseconds).

Input size (no.columns)	1 column full shared memory
2^{23} (2^{17})	267.2
2^{22} (2^{16})	126.4
2^{21} (2^{15})	61.6
2^{20} (2^{14})	30.9

Table 8: Execution times of SP for different number of cycles, number of inputs: 524288, number of columns: 8192 (miliseconds).

Number of cycles	GPGPU	CPU (1 core)
20	2.9	300
40	4.3	555
70	5.7	900
100	6.88	1300

(C implementation). The python implementation is highly inefficient, more than 50-1000 times slower than others (from not vectorized CPU to GPU implementation). The speedups in case of CPU are close to linear. The GPU implementation is significantly faster than in multicore CPU (up to 40-50 times).

Table 9: Execution times of SP for different number of cycles, number of inputs: 524288, number of columns: 8192 (miliseconds).

Number of cycles	CPU (1 core) (vectorized)	CPU (6 cores) (vectorized)
20	72	24
40	113	41
70	196	69
100	325	100

Table 10: Execution times of SP for different inhibition radius values, number of inputs: 524288, number of columns: 8192 (miliseconds).

Inhibition radius	GPGPU	CPU (1 core)
16	6.2	960
32	6.88	1300
64	7.6	2000

Table 11: Execution times of SP for different inhibition radius values, number of inputs: 524288, number of columns: 8192 (miliseconds).

Inhibition radius	CPU (1 core) (vectorized)	CPU (6 cores) (vectorized)
16	261	66
32	325	100
64	444	147

Tables 6 and 7 depict results in case of three different GPU spatial pooler configurations. The last four tables 8, 9, 10, 11 show times of execution in case of different number of learning cycles and inhibition radius value (the one column processed per thread version is described in these tables).

Inhibition radius change has major impact of computations in case of CPU and should be taken into account when the overall execution time is considered, Tab. 6. The simulations were run on NVIDIA Tesla M2090 and Intel Xeon 4565 2.7Ghz. All results presented in tables are average values collected in five measure probes (standard deviation less than 10% of average values).

8 CONCLUSIONS

Our research shows that high level implementation of HTM in object languages is highly inefficient. The C language code run in parallel hardware platform gives significant speedup. It was observed that in case of vectorized and multicore implementation speed up is close to linear. The GPGPU outperforms 6-core CPU. It is worth to say that results measured on CPU with

more cores should be compared with GPU. Therefore performance tests of Spatial Pooler on Xeon Phi will be provided. Our work shows that HTM in hardware accelerators can be used in real-time applications. Further research, will concentrate on parallel GPU and multicore Temporal Pooler implementation. Additionally, adaption of C source code to OpenCL should be done to test in other platforms like FPGA and other heterogenous platforms (Vyas and Zaveri, 2013). At the end comparative studies of efficiency and learning quality should be done among other parallel deep learning models.

ACKNOWLEDGEMENTS

This research is supported by the European Regional Development Program no. POIG.02.03.00-12-137/13 PL-Grid Core.

REFERENCES

- Cai, X., Xu, Z., Lai, G., Wu, C., and Lin, X. (2012). Gpu-accelerated restricted boltzmann machine for collaborative filtering. *ICA3PP'12 Proceedings of the 12th international conference on Algorithms and Architectures for Parallel Processing - Volume Part I*, pages 303–316.
- Cisco (2012). Visual networking index. Visual Networking Index, Cisco Systems.
- Hawkins, J. and Ahmad, S. (2011). Numenta, white paper. Numenta, Hierarchical Temporal Memory, white paper, version 0.2.1, september 12, 2011.
- Hilbert, M. and Lopez, P. (2011). The worlds technological capacity to store, communicate, and compute information. In *University of Vermont, Vol. 332, no. 6025*, pages 60–65.
- Idc (2011). Idc predicts. IDC Predicts 2012 Will Be the Year of Mobile and Cloud Platform Wars as IT Vendors Vie for Leadership While the Industry Redefines Itself. IDC. 2011-12-01.
- Kapuscinski, T. (2010). Using hierarchical temporal memory for vision-based hand shape recognition under large variations in hands rotation. *10th International Conference, ICAISC 2010, Zakopane, Poland, in Artificial Intelligence and Soft Computing, Springer-Verlag*, pages 272–279.
- Lopes, N., Ribeiro, B., and Goncalves, J. (2012). Restricted boltzmann machines and deep belief networks on multi-core processors. *Neural Networks (IJCNN), The 2012 International Joint Conference on*, pages 1–7.
- Numenta (2011). Nupic application. <https://github.com/numenta/nupic/wiki>.
- NVIDIA (2014). Cuda framework. <https://developer.nvidia.com/cuda-gpus>.
- OpenMP (2010). Openmp library. <http://www.openmp.org>.
- Sherwin, J. and Mavris, D. (2009). Hierarchical temporal memory algorithms for understanding asymmetric warfare. *Aerospace conference, 2009 IEEE, MT*, pages 1–10.
- Vyas, P. and Zaveri, M. (2013). Verilog implementation of a node of hierarchical temporal memory. *Asian Journal of Computer Science and Information Technology, AJCSIT*, 3:103–108.
- Wu, X., Zhu, X., Wu, G.-Q., and Ding, W. (2014). Data mining with big data. *Knowledge and Data Engineering, IEEE Transactions on*, 26(1):97–107.